AD-A112 146 ANALYTICAL METHODS INC REDMOND WA F/G 20/4
A SEPARATION MODEL FOR TWO-DIMENSIONAL AIRFOILS IN TRANSONIC FL--ETC(U)
JAN 82 F A DVORAK, D H CHOI DAAG29-78-C-0004
UNCLASSIFIED ARO-15866.2-E NL

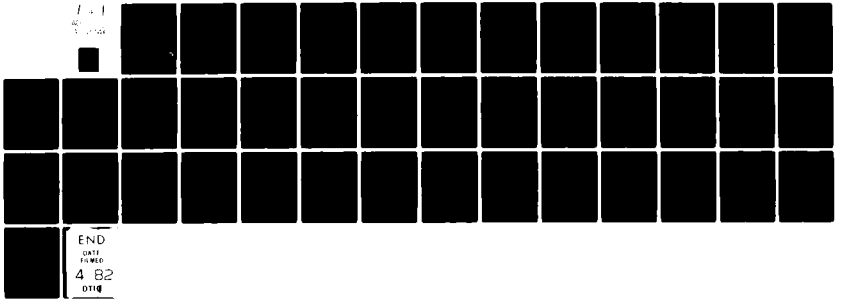

END
DATE FILMED
4 82
DTIC

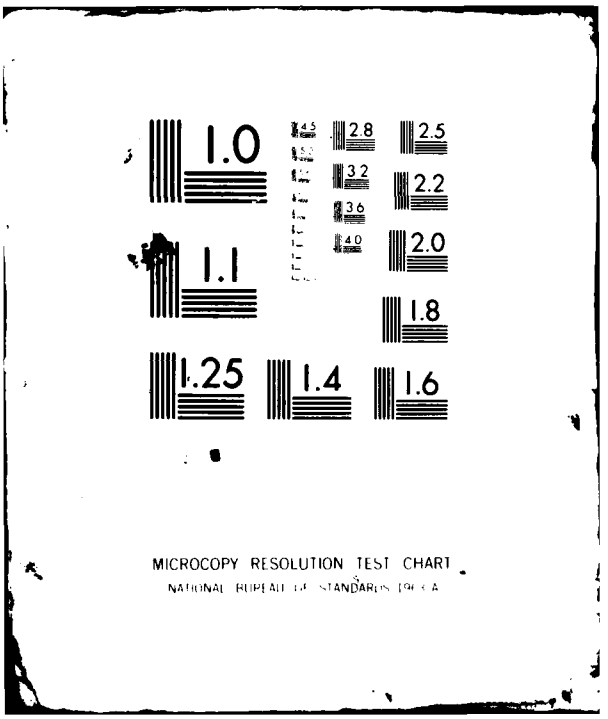
1.0
1.1
1.25
1.4
1.6
1.8
2.0
2.2
2.5
2.8
3.2
3.6
4.0
MICROCOPY RESOLUTION TEST CHART
NATIONAL BUREAU OF STANDARDS 1963 A

ARO .15866.2-E

(12)

FINAL TECHNICAL REPORT

"A SEPARATION MODEL FOR TWO-DIMENSIONAL AIRFOILS IN TRANSONIC FLOW"

DR. F.A. DVORAK

DR. D.H. CHOI

JANUARY 1982

PREPARED FOR:

DEPARTMENT OF THE ARMY
U.S. ARMY RESEARCH OFFICE
P.O. BOX 12211
RESEARCH TRIANGLE PARK, N.C. 27709

UNDER CONTRACT DAAG29-78-C-0004

PREPARED BY:

ANALYTICAL METHODS, INC.
2047 - 152ND AVENUE N.E.
REDMOND, WASHINGTON 98052
(206) 643-9090

Unclassified

SECURITY CLASSIFICATION OF THIS PAGE (When Data Entered)

REPORT DOCUMENTATION PAGE		READ INSTRUCTIONS BEFORE COMPLETING FORM
1. REPORT NUMBER	2. GOVT ACCESSION NO. AD-A112 146	3. RECIPIENT'S CATALOG NUMBER
4. TITLE (and Subtitle) A Separation Model for Two-Dimensional Airfoils in Transonic Flow		5. TYPE OF REPORT & PERIOD COVERED Final Technical Report 15 Nov. 1978 - 30 Nov. 1981
		6. PERFORMING ORG. REPORT NUMBER
7. AUTHOR(s) Dr. Frank A. Dvorak Dr. D.H. Choi		8. CONTRACT OR GRANT NUMBER(s) DAAG29-78-C-0004
9. PERFORMING ORGANIZATION NAME AND ADDRESS Analytical Methods, Inc. 2047 - 152nd Avenue N.E. Redmond, Washington 98052		10. PROGRAM ELEMENT, PROJECT, TASK AREA & WORK UNIT NUMBERS
11. CONTROLLING OFFICE NAME AND ADDRESS U.S. Army Research Office Post Office Box 12211 Research Triangle Park, N.C. 27709		12. REPORT DATE January 1982
		13. NUMBER OF PAGES 38
14. MONITORING AGENCY NAME & ADDRESS(if different from Controlling Office)		15. SECURITY CLASS. (of this report) Unclassified
		15a. DECLASSIFICATION/DOWNGRADING SCHEDULE

16. DISTRIBUTION STATEMENT (of this Report)

Approved for public release; distribution unlimited.

17. DISTRIBUTION STATEMENT (of the abstract entered in Block 20, if different from Report)

18. SUPPLEMENTARY NOTES

The view, opinions, and/or findings contained in this report are those of the author(s) and should not be construed as an official Department of the Army position, policy or decision, unless so designated by other documentation.

19. KEY WORDS (Continue on reverse side if necessary and identify by block number)

separated flows; transonic flow; aerodynamic stall; viscous potential flow interaction analysis

20. ABSTRACT (Continue on reverse side if necessary and identify by block number)

A calculation method for transonic separated flow about two-dimensional airfoils at incidence is presented in this report. The method is capable of predicting the effects of both leading- and trailing-edge separated flows, although the former is usually associated with a complete collapse of the airfoil flow field, in which case the flow is no longer supercritical. A viscous potential flow iteration procedure provides the connection between potential flow, boundary layer and wake modules. The separated wake is modelled in the

DD FORM 1 JAN 73 1473 EDITION OF 1 NOV 65 IS OBSOLETE

Unclassified

SECURITY CLASSIFICATION OF THIS PAGE (When Data Entered)

potential flow analysis by thin sheets across which exists a jump in velocity potential. These sheets are analogous to vorticity sheets in incompressible flow. The basic potential flow method is a modification of Jameson's full potential method. Calculations for four different airfoils have been compared with experiment for pressure distributions as well as integrated forces. The agreement between theory and experiment is generally good even when shock waves are present.

SUMMARY

A calculation method for transonic separated flow about two-dimensional airfoils at incidence is presented in this report. The method is capable of predicting the effects of both leading- and trailing-edge separated flows, although the former is usually associated with a complete collapse of the airfoil flow field, in which case the flow is no longer supercritical. A viscous potential flow iteration procedure provides the connection between potential flow, boundary layer and wake modules. The separated wake is modelled in the potential flow analysis by thin sheets across which exists a jump in velocity potential. These sheets are analogous to vorticity sheets in incompressible flow. The basic potential flow method is a modification of Jameson's full potential method. Calculations for four different airfoils have been compared with experiment for pressure distributions as well as integrated forces. The agreement between theory and experiment is generally good even when shock waves are present.

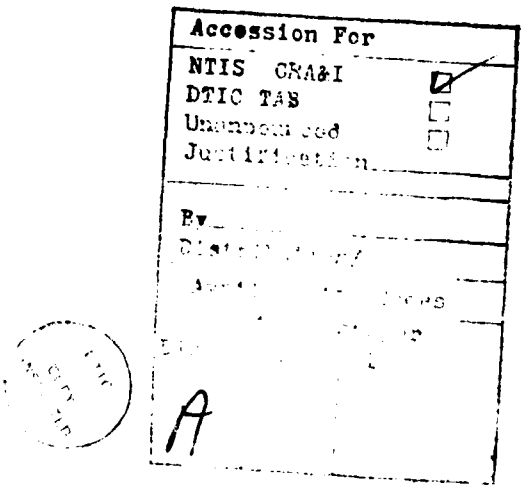

PREFACE

The work described in this technical report was performed by Analytical Methods, Inc. for the Department of the Army, U.S. Army Research Office, Research Triangle Park, North Carolina, under Contract DAAG29-78-C-0004. The research program was undertaken under the technical cognizance of Dr. Robert E. Singleton, Director, Engineering Sciences Division, U.S. Army Research Office. Dr. Frank A. Dvorak was the Principal Investigator and the Program Manager, and Dr. D.H. Choi was an Associate Investigator.

Analytical Methods, Inc. wishes to gratefully acknowledge the assistance of Hughes Helicopters, Inc., Culver City, California, in providing realistic helicopter airfoil geometries for comparison with program TRANMAX.

TABLE OF CONTENTS

LIST OF ILLUSTRATIONS

1.0 INTRODUCTION

A calculation method for transonic separated flow about two-dimensional airfoils at incidence is presented in this report. This aspect of aerodynamics has had relatively little attention, although its importance cannot be overstated. Separated flow is present in almost all applications of practical interest, and a full analysis has not yet been very successful. This is indeed a challenging problem that requires not only a good inviscid transonic flow calculation method, but also an accurate prediction of boundary layer development. Above all, in order to obtain efficiently any realistic solutions for which the large separated region exists, the wake region must be modelled appropriately.

Only a few investigators have attempted to model this complicated flow. Hicks (Ref. 1) has coupled an optimization technique to an existing two-dimensional transonic airfoil code. He has been able to obtain separation profiles where the pressure remains constant along the separating streamline. Unfortunately, this procedure has not yet resulted in good agreement with experimental data. Diewert (Ref. 2) has treated the two-dimensional airfoil with separation using a time-dependent Navier-Stokes code. Initial results for an 18% thick circular arc airfoil with a very small amount of trailing-edge separation are quite good; however, as the separated region increases, agreement with experiment deteriorates. Recently, Barnwell (Ref. 3) proposed a calculation procedure for transonic flow with small amounts of trailing-edge separation. This method employs a closed form solution of the boundary layer equations in the reverse flow region. Limited comparisons with experiment show excellent agreement. Experience with a similar procedure developed by Cousteix (Ref. 4) suggests that this approach can be successful for airfoils with small regions of separated flow, but must break down at large angles of attack where wake modelling becomes important.

---

(1) Hicks, R., Private communication, 1977.

(2) Deiwert, G.S., "Computation of Separated Transonic Turbulent Flows", AIAA Paper 75-829, June 1975.

(3) Barnwell, R.W., "A Potential Flow/Boundary Layer Method for Calculating Subsonic and Transonic Airfoil Flow with Trailing-Edge Separation", NASA TM-81850, June 1981.

(4) Cousteix, J., AFOSR-HTTM-Stanford Conference on: Complex Turbulent Flows, Comparison of Computation and Experiment, Volume I, Stanford University, September 1981.

The purpose of the present work is the development of an analysis method for predicting the performance of two-dimensional airfoils in transonic flow with the main emphasis placed on its modelling of the separated region. It is important to note that a similar method for incompressible flow, CLMAX, developed under Army Research Office support (Contract DAAG29-76-C-0019, Ref. 5) has been very successful in predicting the performance of two-dimensional airfoils having large regions of separated flow. In CLMAX, the wake surface is represented by a constant-strength vortex sheet which, through iteration, assumes a force-free wake position. In the calculation method presented here, TRANMAX, the wake surface is modelled by a discontinuity sheet with constant $-\frac{\partial \phi}{\partial s}$ along it and with a jump in ϕ (tangential velocity) across it. This approach is analogous to the constant strength vorticity sheet model, CLMAX. The wake model in the present code is closed and the shape remains fixed through one complete inviscid flow iteration cycle.

Jameson's code, FL06 (Ref. 6), with substantial change to include the wake region, is used for the inviscid flow calculation. The Cohen-Reshotko (Ref. 7) laminar boundary layer method and Green's (Ref. 8) turbulent lag-entrainment boundary layer method are employed for the viscous flow calculations. The details of the procedure and its performance are described in subsequent sections.

---

(5) Dvorak, F.A., Maskew, B. and Rao, B.M., "An Investigation of Separation Models for the Prediction of $C_{\ell_{max}}$", Final Technical Report, Contract DAAG29-76-C-0019, Prepared for the U.S. Army Research Office, Research Triangle Park, N.C., April 1979.

(6) Jameson, A., "Numerical Computation of Transonic Flows with Shock Waves", International Union of Theoretical and Applied Mechanics, Springer-Verlag New York, Inc., September 1975, pp. 384-414.

(7) Brune, G.W. and Manke, J.W., "An Improved Version of the NASA Lockheed Multielement Airfoil Analysis Computer Program", NASA CR-15323, March 1978, pp. 69-87.

(8) Green, J.E., Weeks, D.J. and Brooman, J.W.F., "Prediction of Turbulent Boundary Layers and Wakes in Compressible Flow by a Lag-Entrainment Method", Royal Aircraft Establishment TR-72231, December 1972.

2.0 DESCRIPTION OF THE ANALYSIS METHOD

2.1 General Description

The present analysis method is built upon Jameson's two-dimensional potential flow calculation method (Ref. 6), FL06, Cohen/Reshotko's laminar boundary layer method (Ref. 7) and Green's lag-entrainment turbulent boundary layer method (Ref. 8). These methods were verified thoroughly by their originators and can be used for transonic flow calculations with confidence.

The solution procedure is shown in Figure 1. The initial potential flow solution is obtained either with or without the wake prescribed, depending on the initial separation point. The potential flow method has been substantially modified to model the separation region with the shape of the wake generated by a procedure to be described in a later section. Having obtained the inviscid pressure distribution, the boundary layer development is predicted using the methods mentioned earlier. This completes one viscid/inviscid calculation cycle.

In subsequent iterations, the induced normal velocity on the airfoil surface due to boundary layer displacement effect is taken into account. A new wake is generated at the start of every iteration.

This procedure is repeated until the solution converges; i.e., the separation points between two successive iterations remain unchanged.

Details of individual elements are fully described in the following sections.

2.2 Potential Flow Calculation Method

2.2.1 Basic Equations

From the equation of continuity and the momentum equation, we have

$$(a^2 - u^2)\frac{\partial u}{\partial x} - uv\left(\frac{\partial u}{\partial y} + \frac{\partial v}{\partial x}\right) + (a^2 - v^2)\frac{\partial v}{\partial y} = 0 \qquad (1)$$

Assuming irrotational flow, a velocity potential, ϕ, can be defined; i.e.,

$$u = \frac{\partial \phi}{\partial x}, \qquad v = \frac{\partial \phi}{\partial y} \qquad (2)$$

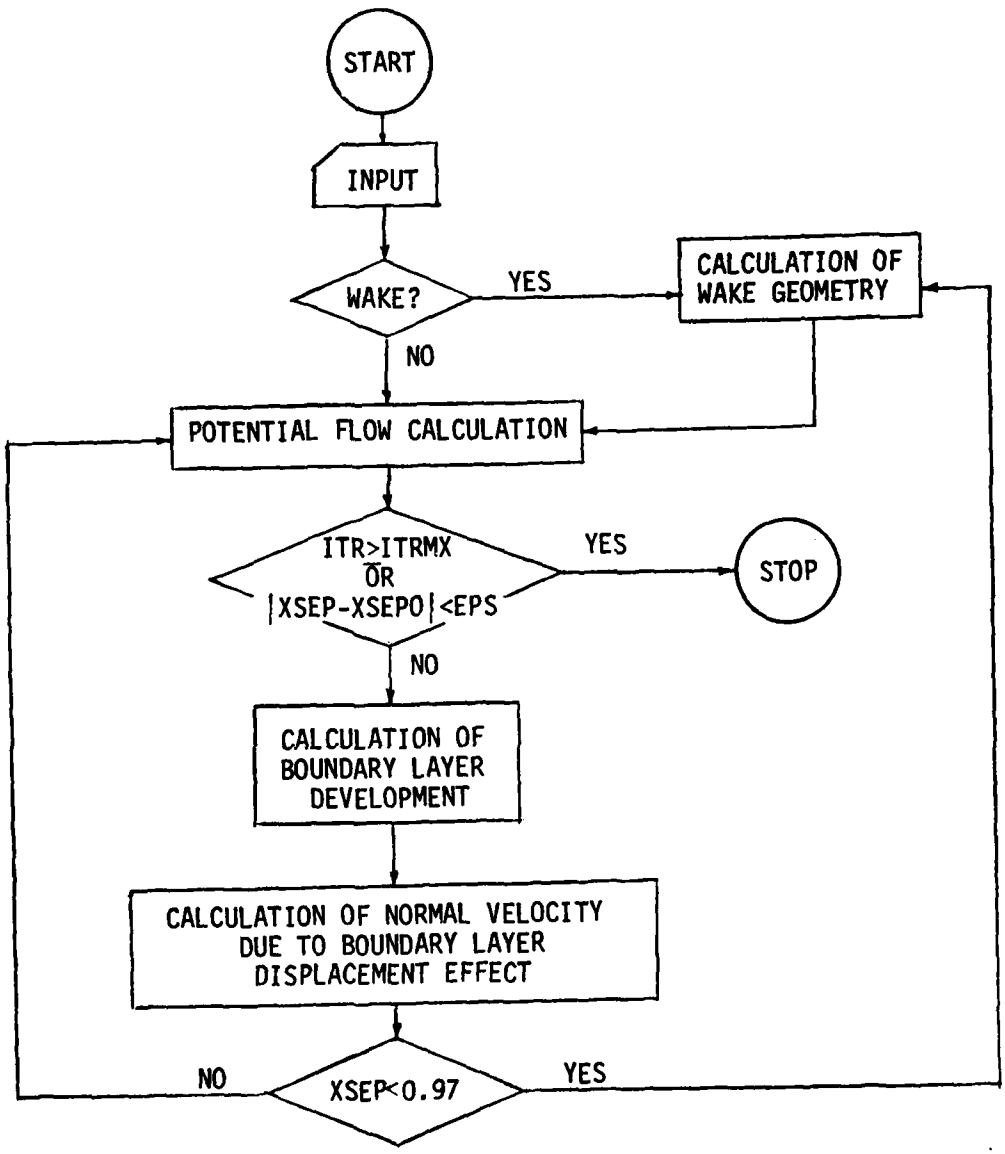

Figure 1. Calculation Procedure.

Substitute these into Eqn. (1) to obtain:

$$(a^2 - u^2)\phi_{xx} - 2uv\phi_{xy} + (a^2 - v^2)\phi_{yy} = 0 \qquad (3)$$

This equation can be solved for ϕ with the use of the energy equation

$$a^2 + \frac{\gamma - 1}{2} q^2 = \left(\frac{1}{M_\infty^2} + \frac{\gamma - 1}{2} \right) q_\infty^2 \qquad (4)$$

where

$$q = \sqrt{u^2 + v^2}$$

The Neumann boundary condition is prescribed along the surface: $\frac{\partial \phi}{\partial n} = 0$, is set initially, and it takes a new value which reflects the viscous effect after each iteration cycle

$$\frac{\partial \phi}{\partial n} = 0 \qquad \text{(First Iteration)}$$

$$\frac{\partial \phi}{\partial n} = \frac{1}{\rho} \frac{\partial}{\partial s}(\rho u \delta^*) = f \qquad \text{(Subsequent Iterations)} \qquad (5)$$

where δ^* is the boundary layer displacement thickness and s is measured along the airfoil surface.

Because of the nature of Eqn. (3), hyperbolic if the local Mach number, $M = q/a > 1$ and elliptic if $M < 1$, it is essential to transform the infinite flow field onto a finite domain. This can be achieved by mapping the exterior of the airfoil in the z-plane conformally onto the interior of a unit circle in the σ-plane as shown in the following figure taken from Reference 9.

---

(9) Rogers, E.O., "Numerical Solution of Subcritical Flow Past Airfoils", NSRDC Report 4112, May 1973.

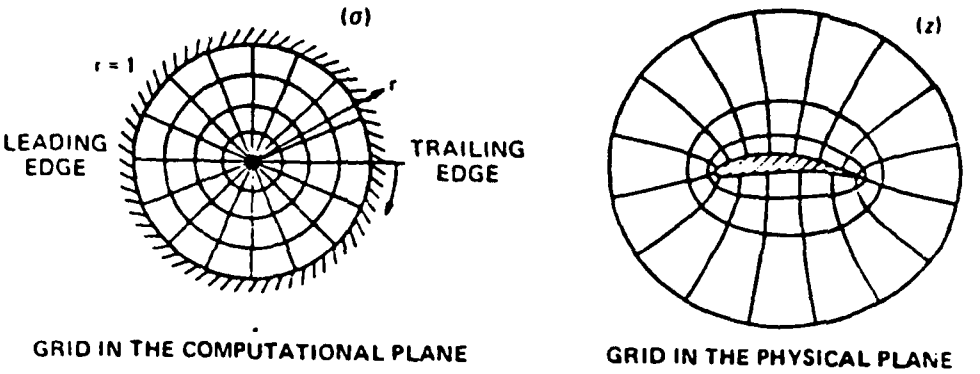

Figure 2. Grid System.

This transformation is particularly useful because an evenly distributed grid system in the circle plane gives denser finite mesh near the body at the leading and trailing edges in the physical plane where it is needed most.

2.2.2 Mapped Coordinate System

Consider the speed in the z-plane,

$$q^2 = u^2 + v^2 = \left|\frac{\partial\phi}{\partial z}\right|^2 = \left|\frac{\partial\phi}{\partial\sigma}\right| /B^2 = \frac{1}{B^2}\left[\left(\frac{\partial\phi}{r\partial\theta}\right)^2 + \left(\frac{\partial\phi}{\partial r}\right)^2\right] \tag{6}$$

where

$$B = \left|\frac{\partial z}{\partial\sigma}\right|$$

Thus we have

$$\frac{\partial\phi}{\partial x} = \frac{\partial\phi}{r\partial\theta}/B, \qquad \frac{\partial\phi}{\partial y} = \frac{\partial\phi}{\partial r}/B \tag{7}$$

The complex potential about a unit circle in a uniform stream is given by:

$$w = U_\infty(z + \frac{1}{z}) + iE\ell nz \tag{8}$$

Here the velocity potential at infinity becomes unbounded and is of the order R. Since the present transformation requires the direct inversion of this external flow, the singular behavior at infinity inevitably occurs at the origin of the σ-plane.

In order to remove this singularity at the origin, $\theta(1/r)$, and the discontinuity at $\theta = 2\pi$ due to the circulation, a translated potential, G, is introduced.

$$G = \phi - \frac{\cos(\theta + \alpha)}{r} + E(\theta + \alpha) \tag{9}$$

where $2\pi E$ is the circulation, and α is the angle of attack.

Substituting Eqns. (7) and (9) into Eqn. (2) to obtain

$$(a^2 - u^2)\, G_{\theta\theta} - 2uvrG_{r\theta} + (a^2 - v^2)\, r \frac{\partial}{\partial r}(rGr)$$

$$- 2uv(G_\theta - E) + (u^2 - v^2)G_r + (u^2 + v^2)(\frac{u}{r} B_\theta + vB_r) = 0 \tag{10}$$

where

$$u = \frac{r(G_\theta - E) - \sin(\theta + \alpha)}{B}, \qquad v = \frac{r^2 G_r - \cos(\theta + \alpha)}{B}$$

The Neumann boundary condition reduces to

$$G_r = \cos(\theta + \alpha) - \frac{f}{B} \qquad \text{at } r = 1 \tag{11}$$

while the far-field boundary condition becomes

$$G = E\left\{\theta + \alpha - \tan^{-1}\left[\sqrt{1 - M_\infty^2}\,\tan(\theta + \alpha)\right]\right\} \qquad \text{at } r = 0 \qquad (12)$$

Here, the circulation constant, E, is determined by the Kutta condition derived from the upper and lower surface separation pressures and is discussed in a later section.

2.2.3 Inviscid Model of Separated Region

As mentioned earlier, the modelling of the wake is one of the most important elements in the method. One may solve the parabolized Navier Stokes equations for the special class of flow instead of modelling the wake. However, this, in principle, cannot handle the region of large reverse flow. On the other hand, solving the full time-dependent Navier Stokes equations is not practical at this time because of the enormous computing time required. The only logical approach to this problem is to simulate the separated flow with an inviscid wake model. A good wake model, in fact, can represent the actual flow very well as was demonstrated by an earlier study (CLMAX).

In the present model, the separated region is confined by two dividing streamlines, one from the upper surface separation point and the other from the trailing-edge point, as shown in Figure 3.

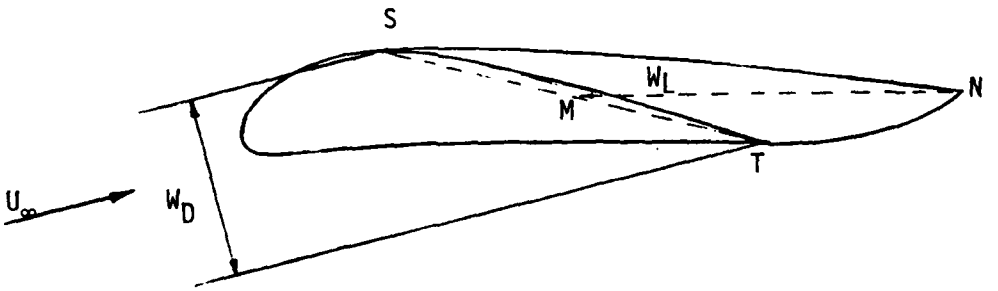

Figure 3. Wake Model.

As shown in the figure, along the dividing streamlines the gradient in velocity potential, $\frac{\partial \phi}{\partial s}$, is constant, while across the streamlines $\frac{\partial \phi}{\partial n}$ is zero.

The wake shape must be updated according to the new separation point. If the separation point remains unchanged, then the solution is considered to be converged.

Construction and Transformation of the Wake

Once the separation point, S, on the upper surface is found, the wake is generated in the following manner (see Figure 3). M is the mid-point on the chord, $\overline{ST}$, and the point, J, is fixed at twice the wake width (W_D) away from the point, M. The slope of $\overline{MN}$ is chosen to be .45 times the trailing-edge slope. Two parabolas can then be constructed through SN and TN, whose initial slopes are equal to the body slopes at their respective points.

This wake in the physical plane can now be transformed onto the circle plane. First, the grid network on the physical plane, which corresponds to the uniform grid in the circle plane, is generated by using the mapping function. With the aid of simple interpolation, the wake in the physical plane can be readily transformed onto the circle plane. A typical resulting separated region in the circle plane is shown in Figure 4.

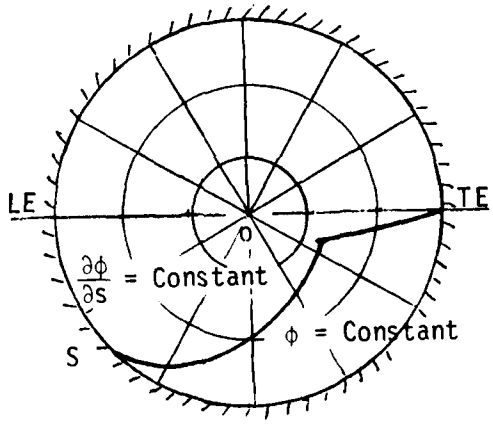

Figure 4. Separated Region in the Computational Plane.

The streamlines which divide the flow into attached and separated flow regions represent lines of constant $\frac{\partial \phi}{\partial s}$. As in the wake model used in Program CLMAX, these streamlines represent thin shear layers across which there exists a a jump in tangential velocity; and, consequently, a jump in velocity potential, ϕ. Due to this jump, a special treatment in the finite-difference scheme is necessary along this boundary. In the present scheme, the value of ϕ is adjusted up or down by the amount of jump, $\Delta\phi$, where

$$\Delta\phi_i = \frac{\partial \phi}{\partial s} \Delta s_i$$

and Δs is measured from point S or T, depending on the particular side, to make the function ϕ continuous across the dividing streamline. With this addition and subtraction, the same difference formulae can be used throughout the field. The procedure is similar to the so-called "shock-fitting" technique.

The Kutta condition, which is normally applied at the trailing edge, is applied at points S and T; i.e.,

$$\left.\frac{\partial \phi}{\partial s}\right|_S = \left.\frac{\partial \phi}{\partial s}\right|_T \tag{13}$$

Special Treatment in Finite-Difference Formulae Along the Dividing Streamline

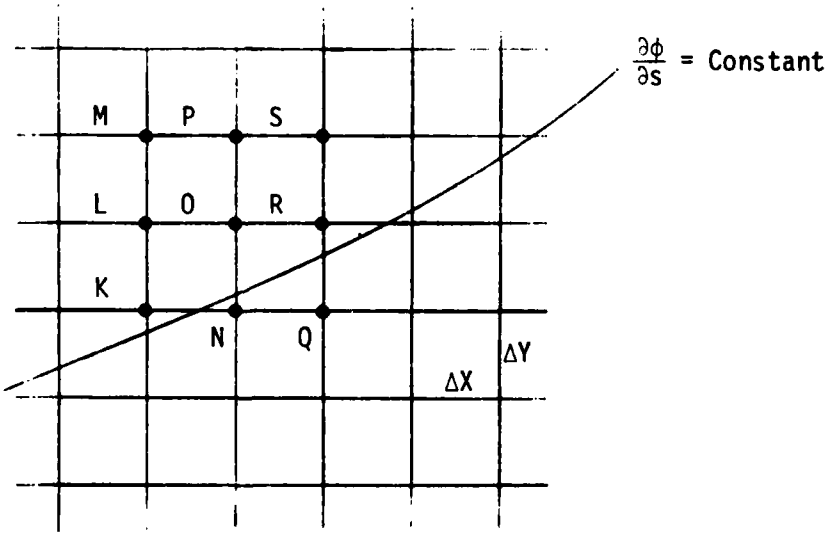

Figure 5. Finite-Difference Grid.

The main idea of present finite-difference formulae near the dividing streamline is to make the potential, ϕ, continuous across this streamline. As previously mentioned, this can be achieved by adding or subtracting the amount of jump, $\Delta\phi$, to or from ϕ at a particular point. The correction is applied to all points lying on the side opposite the point of finite-difference approximation.

As for examples, the derivatives about the point, O, are shown below.

$$\partial\phi/\partial x = (\phi_R - \phi_L)/(2 \cdot \Delta x) \qquad (14(a))$$

$$\partial\phi/\partial Y = \Big(\phi_P - (\phi_N - \Delta\phi_N)\Big)/(2 \cdot \Delta Y) \qquad (14(b))$$

where $\Delta\phi_N = \left.\frac{\partial\phi}{\partial s}\right|_{\text{at separation}} \cdot \Delta s_N$

Δs_N = arc length along the dividing streamline

$$\partial^2\phi/\partial X^2 = (\phi_R - 2\phi_O + \phi_L)/\Delta x^2 \qquad (14(c))$$

$$\partial^2\phi/\partial Y^2 = \Big(\phi_P - 2\phi_O + (\phi_N - \Delta\phi_N)\Big)/\Delta Y^2 \qquad (14(d))$$

$$\partial^2\phi/\partial X\partial Y = \Big(\phi_S - \phi_M + \phi_K - (\phi_Q + \Delta\phi_Q)\Big)/4(\Delta X \Delta Y) \qquad (14(e))$$

2.2.4 Method of Solution

The transformed Eqn. (10) with boundary conditions, Eqns. (11) and (12), is solved by a finite-difference scheme. Upwind differencing is used when the local flow is supersonic , while central difference formulae are used at subsonic points. The resulting set of difference equations is solved iteratively. Details of the method are referred to in the original paper (Ref. 6) and only the major differences are presented here.

The Kutta condition is imposed by matching the pressures at the upper surface separation point and the trailing edge; i.e.,

$$\left.\frac{\partial\phi}{\partial s}\right|_{\text{sep}} = \left.\frac{\partial\phi}{\partial s}\right|_{\text{trailing edge}} \qquad (13)$$

The amount of circulation, E, in Eqn. (9) is continuously updated to satisfy Eqn. (13). The new estimate of E, determined from the Kutta condition, is then used for the next iteration. This cycle is repeated until the correction to E satisfies the convergence criteria.

It was found, during the course of this work, that the method may encounter some difficulty if the solution is sought directly for free stream Mach numbers greater than 0.35. This occurs because the actual flow is becomming less stable and will respond rapidly to even small disturbances. When the separation region is large (greater than 10% chord), the initial inviscid flow field is not representative of the flow field with separation; consequently, a poor initial solution can lead to divergent behavior at higher Mach numbers. Proper convergence and stability can be achieved by starting the solution from a low Mach number and raising the Mach number incrementally to the desired value.

After the translated potential, G, is obtained, the tangential velocity component, u, on the surface can be obtained readily through simple differencing. The pressure coefficient, C_p, along the surface is given by:

$$C_p = \frac{1}{\frac{\gamma}{2} M_\infty^2} \left\{ \left[1 + \frac{\gamma - 1}{2} M_\infty^2 (1 - u^2) \right]^{\frac{\gamma}{\gamma - 1}} - 1 \right\} \qquad (15)$$

2.3 Calculation of Boundary Layer Development

As in the potential flow calculation procedure, new methods for both laminar and turbulent boundary layers were adopted. Curle's method for laminar flow and the Nash-Hicks method for turbulent flow are replaced by the Cohen-Reshotko method and Green's method, respectively. However, the same transition criterion, the Granville procedure, is still intact. The possibility of the reattachment as a turbulent boundary layer after laminar boundary layer separation is also examined on the basis of the Reynolds number based on the momentum thickness at the point of separation (Ref. 10).

2.3.1 Cohen and Reshotko Method

This integral method was developed for the steady two-dimensional laminar boundary layer with the assumption that the surface temperature is uniform.

---

(10) Dvorak, F.A. and Woodward, F.A., "A Viscous/Potential Flow Interaction Analysis Method for Multi-Element Infinite Swept Wings; Volume I", NASA CR-2476, November 1974.

First, consider the Stewartson transformation,

$$\frac{\partial \psi}{\partial y} = \frac{\rho u}{\rho_o}, \qquad \frac{\partial \psi}{\partial x} = \frac{-\rho v}{\rho_o}$$

$$X = \int_o^x \lambda \frac{a_e}{a_o} \frac{P_e}{P_o} dX \qquad Y = \frac{a_e}{a_o} \int_o^y \frac{\rho}{\rho_o} dY$$

$$U = \frac{\partial \psi}{\partial y} \qquad V = - \frac{\partial \psi}{\partial x} \tag{16}$$

where ψ and a represent the stream function and the speed of sound, respectively. Capital letters denote quantities of the equivalent incompressible problem. With this transformation, the equivalent incompressible problem can be formulated. Now, define a parameter,

$$n = - \frac{\theta^2_{tr}}{\nu_o} \frac{dU_e}{dX} \tag{17}$$

where subscript, tr, denotes the transformed coordinate. After some manipulation, one can obtain

$$n = - C_1 M_e^{-C_2} \frac{dM_e}{dx} T_e^{-4} \int_o^x M_e^{C_2 - 1} T_e^4 \, dx \tag{18}$$

where C_1 and C_2 are constants.

This can be readily solved for n by simple integration formulae such as the trapezoidal rule. Then the momentum thickness and the shape factor are obtained from the explicit expressions of n. (See Ref. 7 for details.)

The separation of the boundary layer is detected by examining the Pohlhausen parameter, $\Lambda = \frac{\delta^2}{\nu} \frac{dU}{dx}$, assuming that the H-$\Lambda$ table for the incompressible flow is still valid.

After transition, either through natural transition or through a separation/reattachment process, Green's method takes over the calculation of downstream turbulent boundary layer development.

2.3.2 Green's Method

This is a "lag-entrainment" integral method involving three equations: momentum-integral, entrainment and a rate equation for the entrainment coefficient (Ref. 8). The method is a combination of Head's original entraiment momentum-integral method and the turbulent model proposed by Bradshaw et al. in which the algebraic relation for the entrainment coefficient of Head's method is replaced by a rate equation derived from the turbulent kinetic energy equation.

The resulting equations are:

$$\frac{d\theta}{cx} = \overline{H}_1 \ (\theta, \overline{H}, C_E) \tag{19}$$

$$\frac{d\overline{H}}{dx} = \overline{H}_2 \ (\theta, \overline{H}, C_E) \tag{20}$$

$$\frac{dC_E}{dx} = \overline{H}_3 \ (\theta, \overline{H}, C_E) \tag{21}$$

where

$$\theta = \int_0^\infty \frac{\rho u}{\rho u_e} \left(1 - \frac{u}{u_e}\right) dy$$

$$\overline{H} = \frac{1}{\theta} \int_0^\infty \frac{\rho}{\rho_e} \left(1 - \frac{u}{u_e}\right) dy$$

$$C_E = \frac{1}{\rho_e u_e} \frac{d}{dx} \int_0^\delta \rho u dy$$

This system of ordinary differential equations is solved by the Runge-Kutta method. The separation point can be located by monitoring both the friction coefficient, C_f, and the shape factor, H.

3.0 RESULTS AND DISCUSSION

The main purpose of this analysis method, TRANMX, is to predict the performance of a given airfoil for a wide range of angles of attack, and to determine the maximum lift and its corresponding angle. As will be presented in this section, TRANMX performs very well for all the cases examined. The pressure distributions and the $C_\ell - \alpha$ curves are in excellent agreement with the experimental data.

The method has been tested against four distinctly different airfoils; i.e., GA(W)-1, NACA 0012, Model A1 and a Hughes Helicopter Company airfoil with tab. The free stream Mach number varies from .15 for the GA(W)-1 to .6 for the A1 airfoil. For each flow condition, the angle of attack is gradually increased until the airfoil has stalled. Airfoils at angles of attack beyond the static stall angle have been analysed.

Figure 6(a), (b) and (c) shows the pressure distributions about the airfoil, GA(W)-1, for $M_\infty = 0.15$ and $Re = 6 \times 10^6$. It should be noted that this is the same test case with which the results of CLMAX were in good agreement. The good correlation shown in these figures confirms that these two analytical methods are compatible. The computed C_ℓ is a little higher than the data as shown in Figure 7 due to the slightly higher pressure distribution along the lower surface. However, this discrepancy of less than 3% is well within the experimental accuracy.

The comparisons shown in Figures 8 and 9 are for the NACA 0012 symmetric airfoil at $M_\infty = 0.5$, $Re = 3 \times 10^6$. Here again the results are quite good although the quoted angles of attack appear to be high. It is interesting to note that the pure inviscid solution for $\alpha = 9.86$, which is plotted in Figure 8(c), fails to predict the real pressure distribution by a surprising margin. A separated region of about 20% of the chord makes the pure potential flow solution meaningless. This indicates that the viscid/inviscid interation changes the real flow field considerably and the viscous effects cannot be ignored.

The results of two different calculation methods are plotted in Figure 10 along with experimental data for a Hughes Helicopter Company airfoil. The free stream Mach number is .46 and the Reynolds number is 3.8 million. CLMAX does not perform very well, particularly because it is not developed to handle the highly compressible flow. This also shows the limitation of the usage of linearized equations in compressible flow for this Mach number. TRANMAX performs well except at the highest angle of attack (Figure 10(c)). In this case, the actual flow reaches a local Mach number of 1.5 and the boundary layer is believed to separate at the foot of the shock. This boundary layer (separation) effectively removes the distinct shock but fails to reattach. This separated flow exhibits quite different characteristics, e.g., varying pressure along the body, and cannot be treated as well by the present method. The $C_\ell - \alpha$ curve shown in Figure 11 is, therefore, rather fortuitous where $\alpha > 10°$.

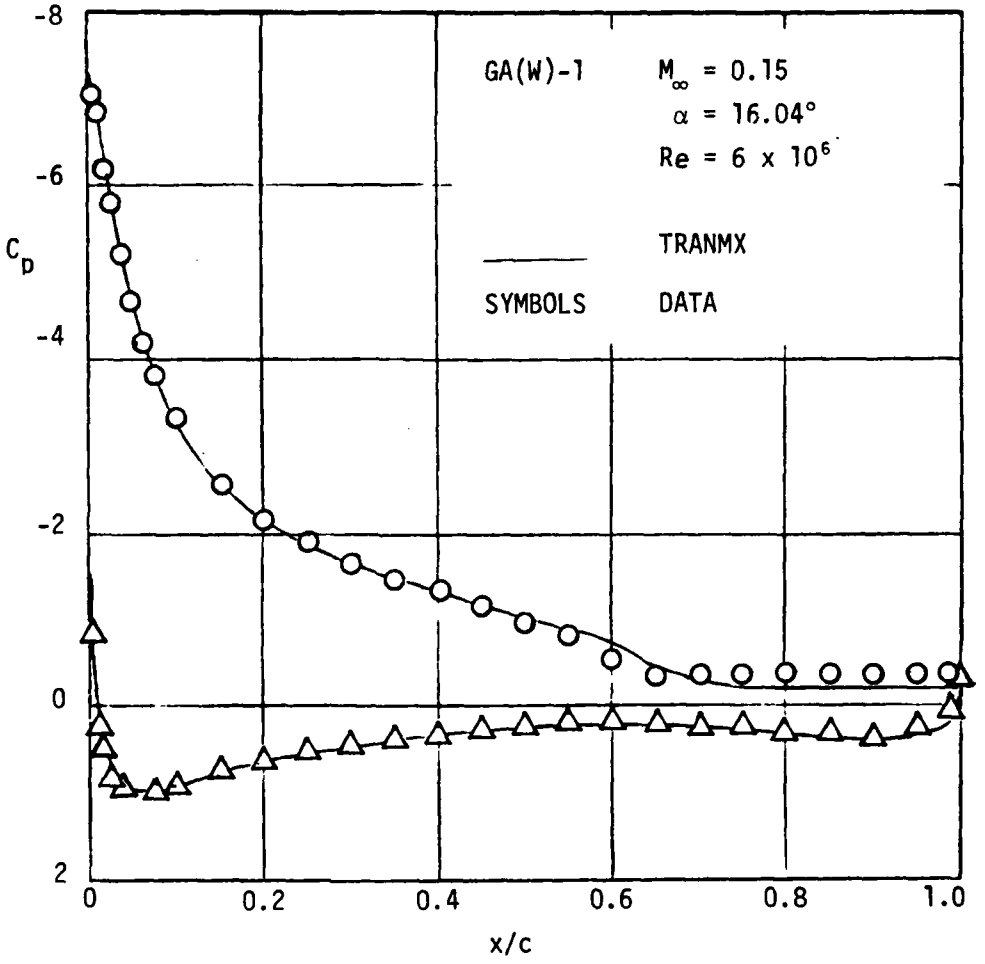

(a)

Figure 6. Pressure Distribution along GA(W)-1 Airfoil.

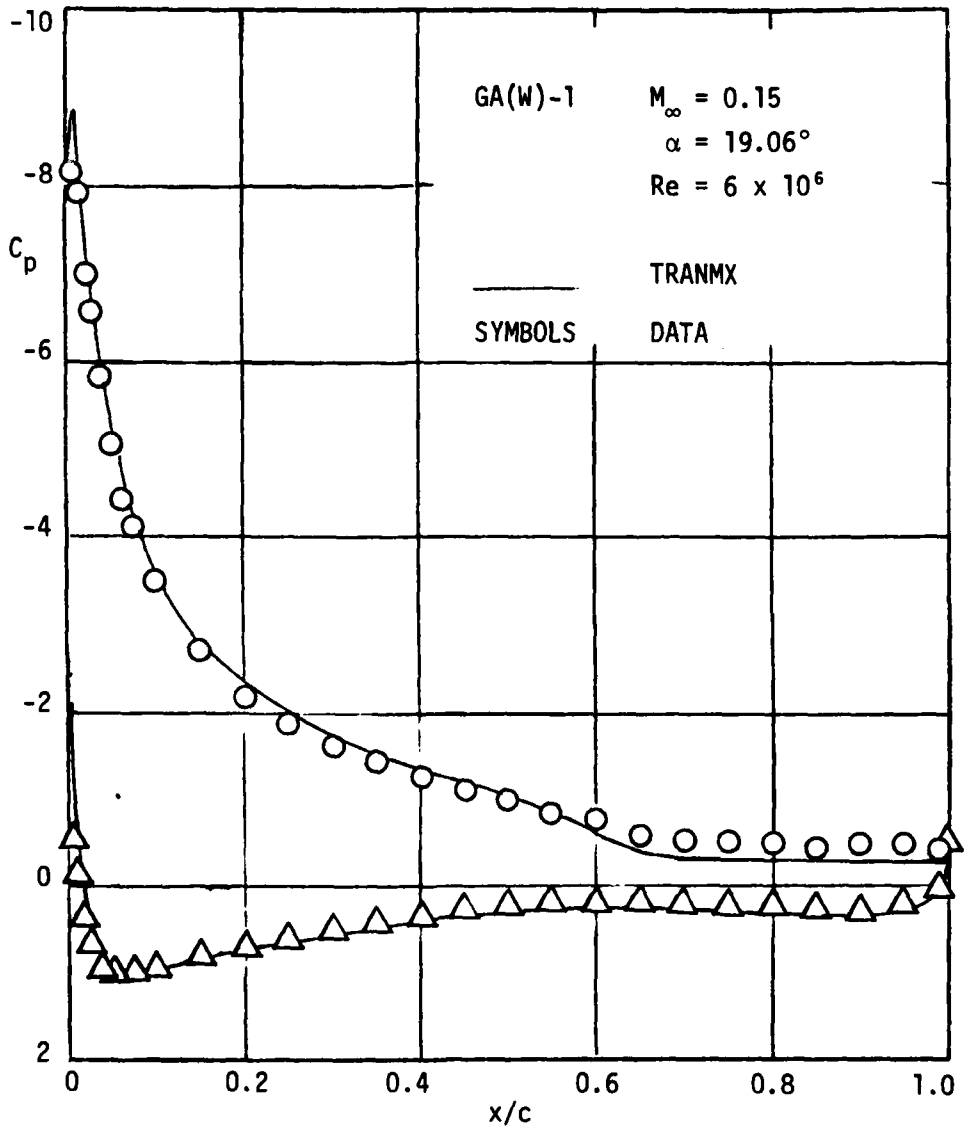

(b)

Figure 6. Continued.

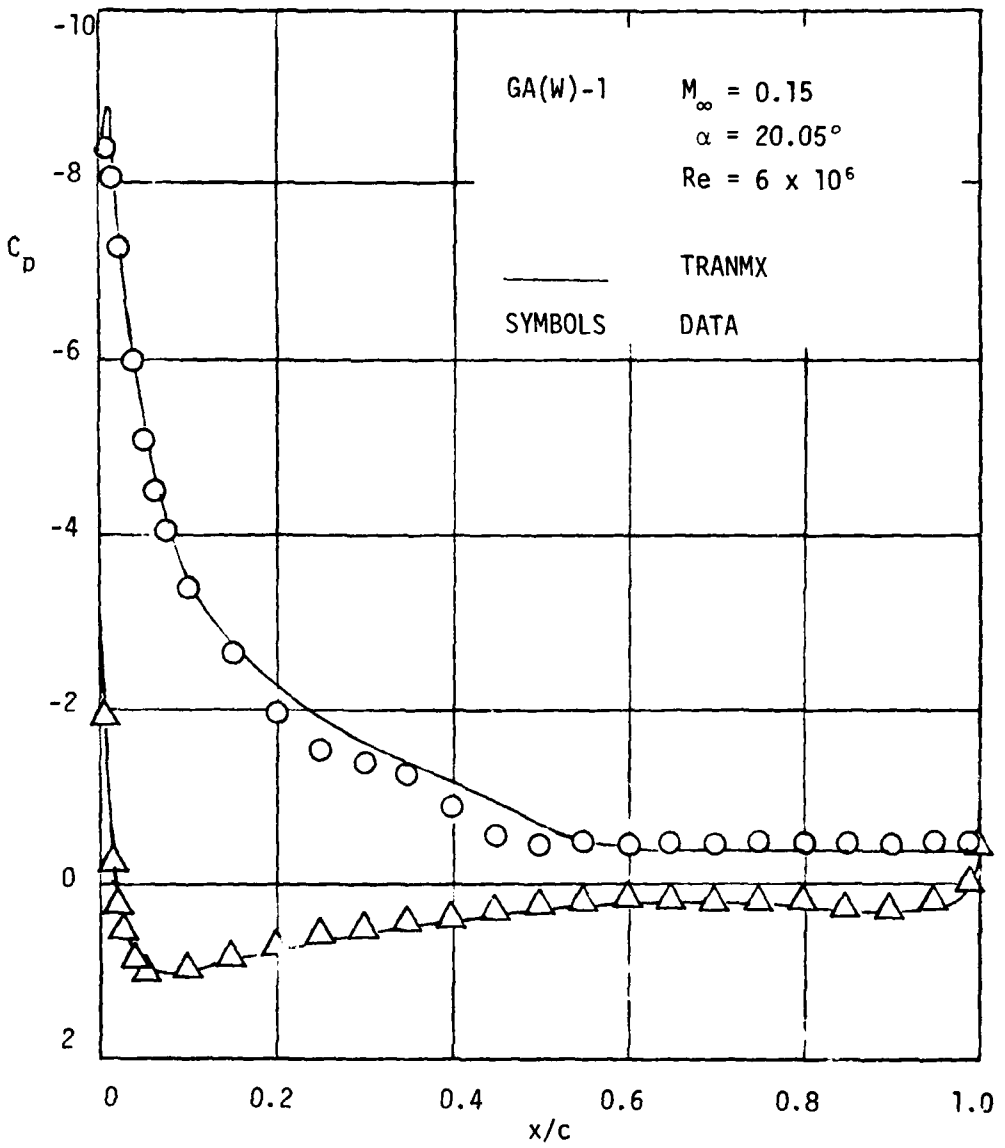

(c)

Figure 6. Concluded.

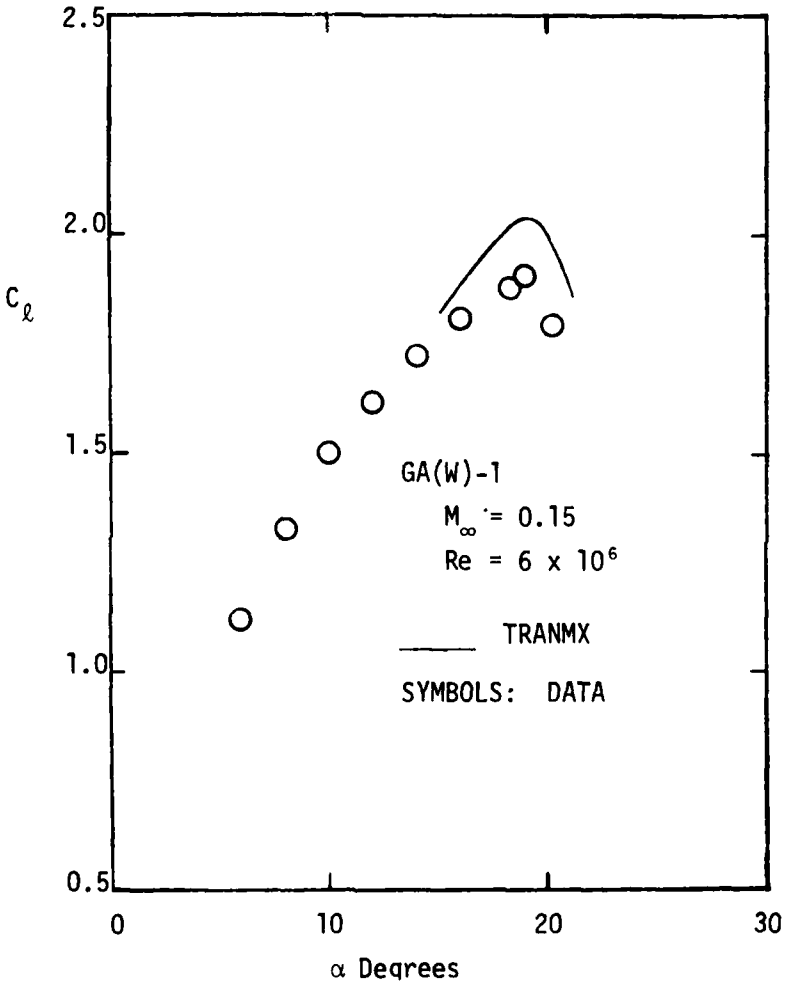

Figure 7. C_ℓ - α Curve for GA(W)-1 Airfoil.

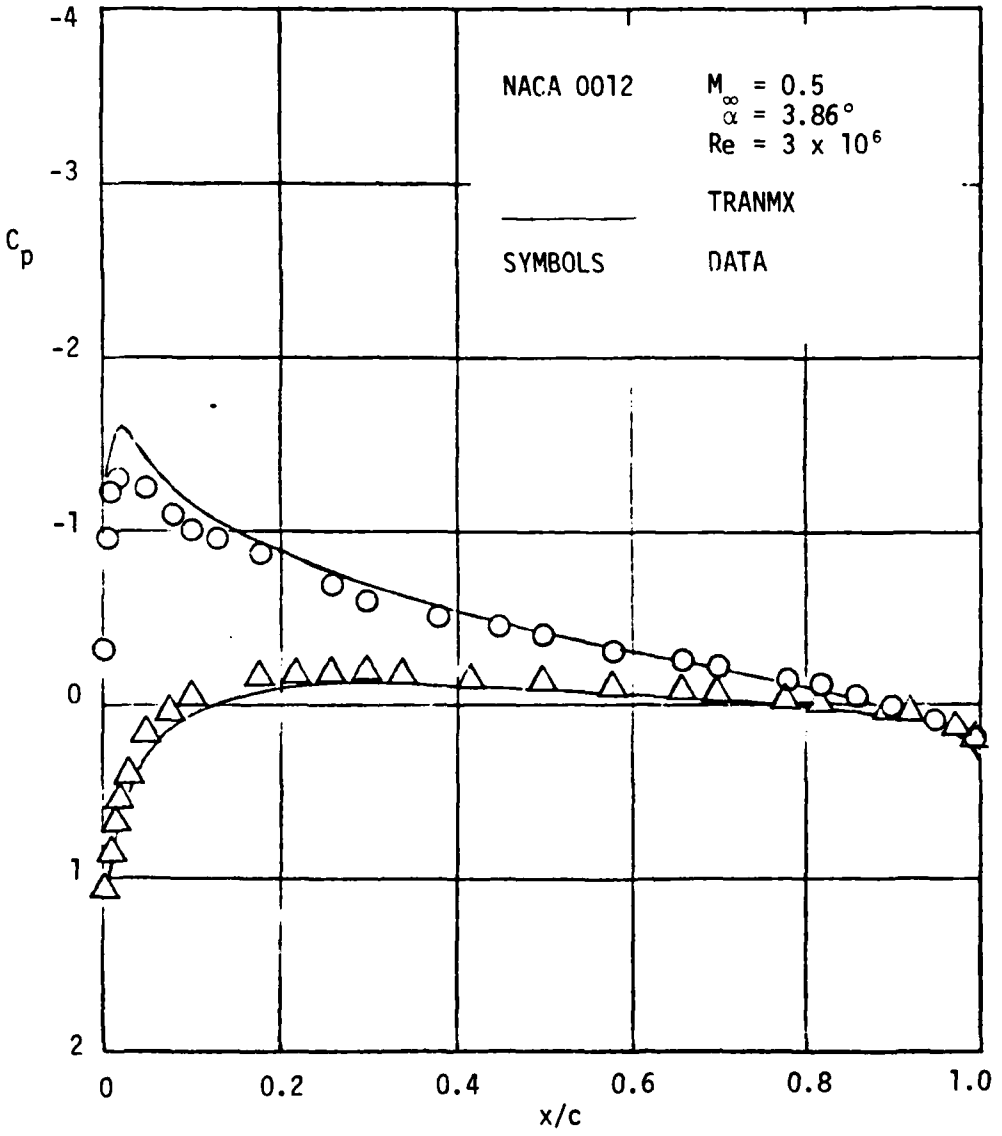

(a)

Figure 8. Pressure Distribution along a NACA 0012.

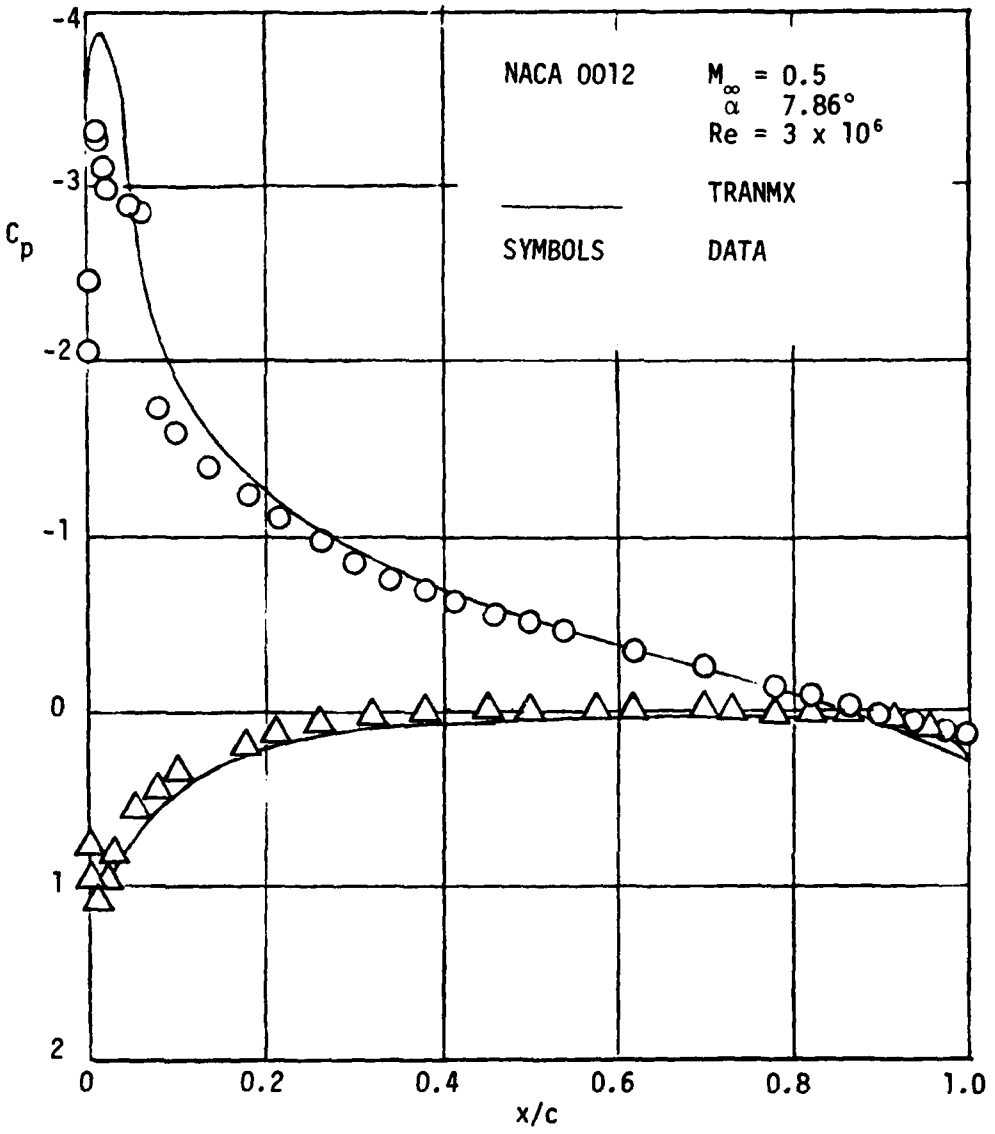

(b)

Figure 8. Continued.

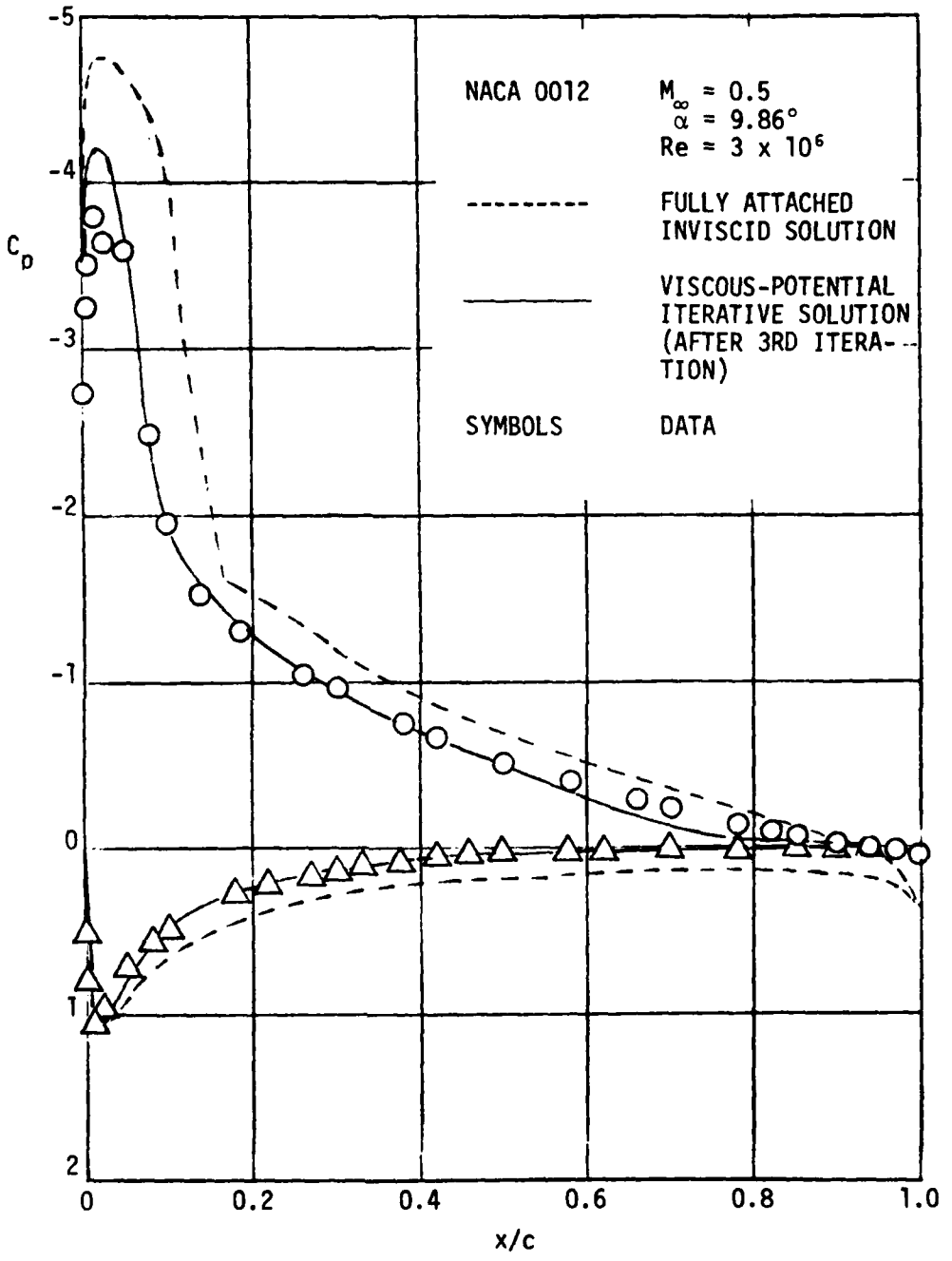

(c)

Figure 8. Concluded.

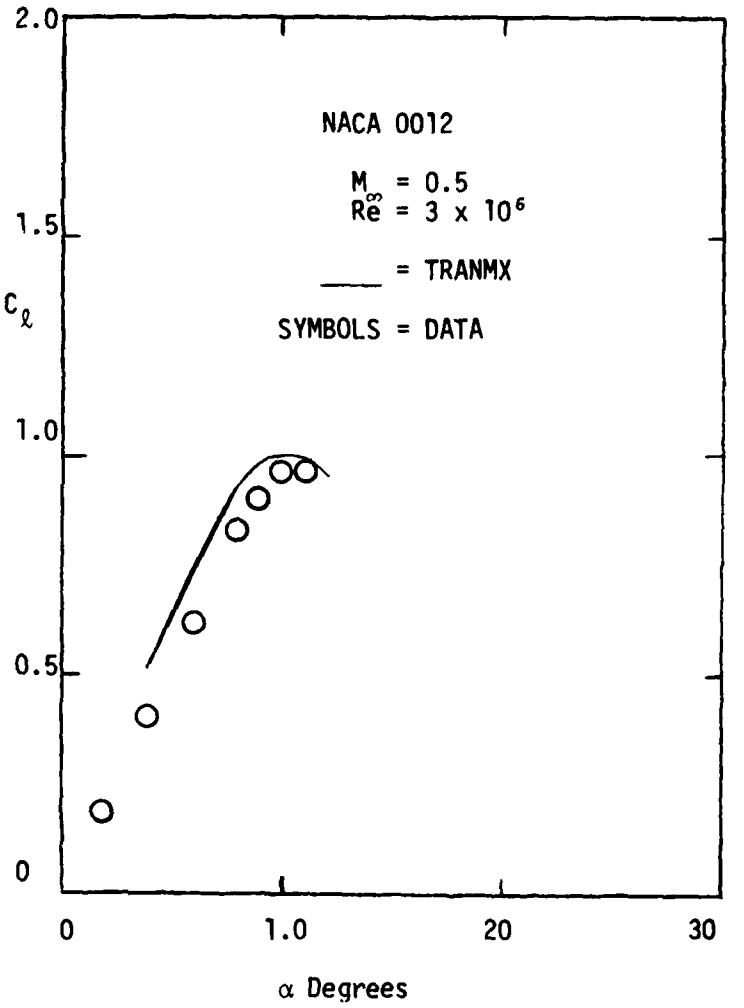

Figure 9. C_ℓ - α Curve for NACA 0012 Airfoil.

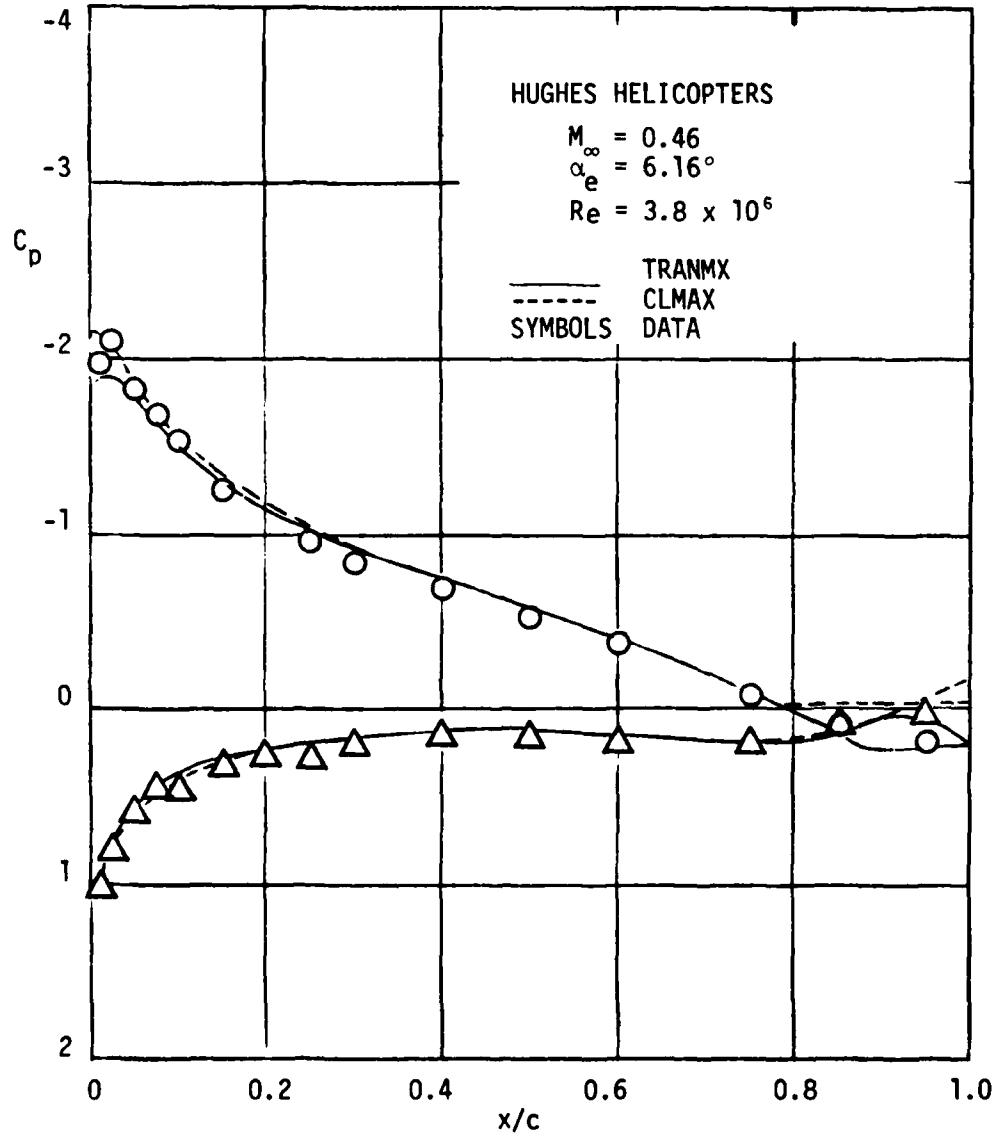

(a)

Figure 10. Pressure Distribution along a Hughes Helicopters Company Airfoil.

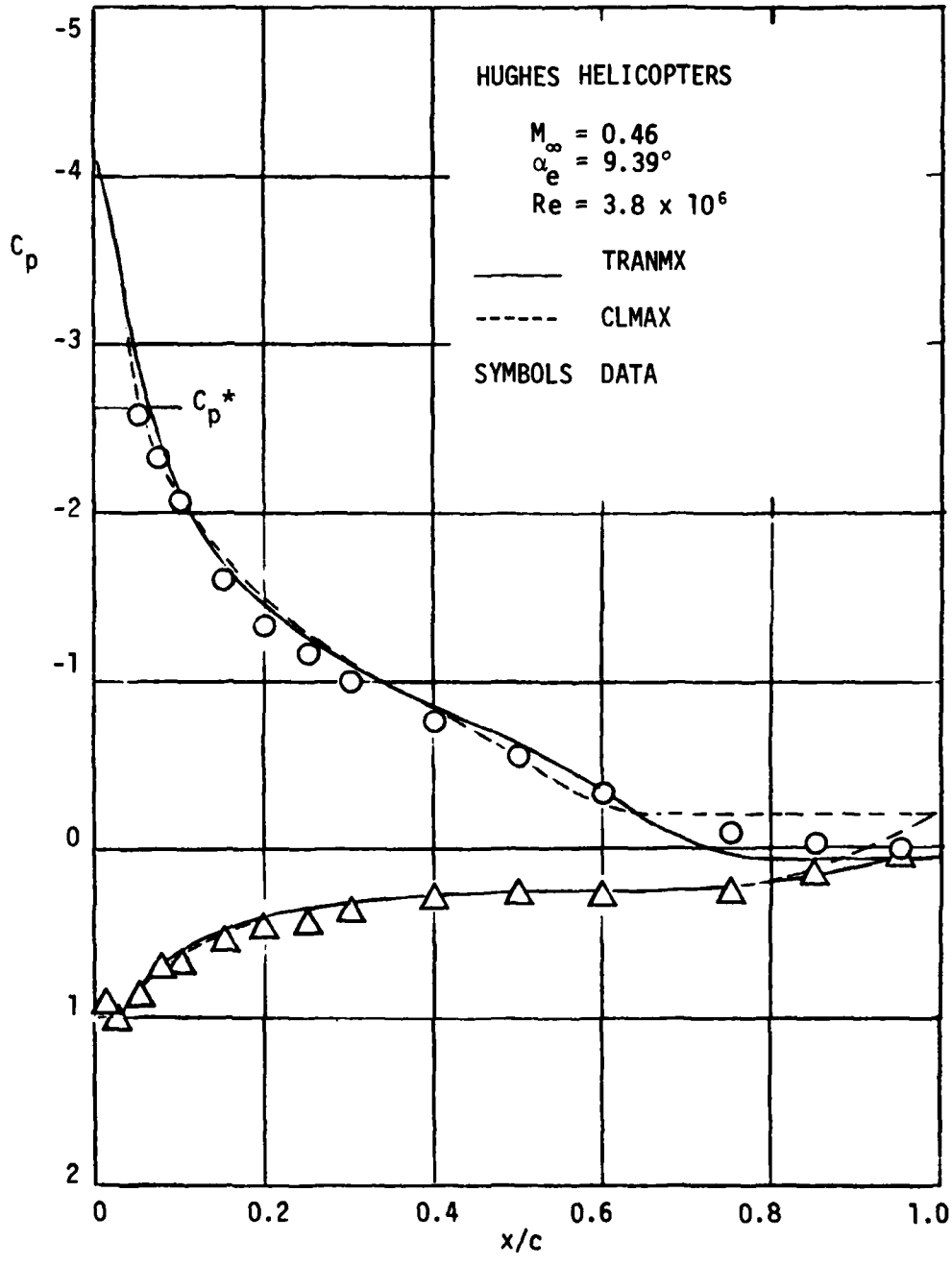

(b)

Figure 10. Continued.

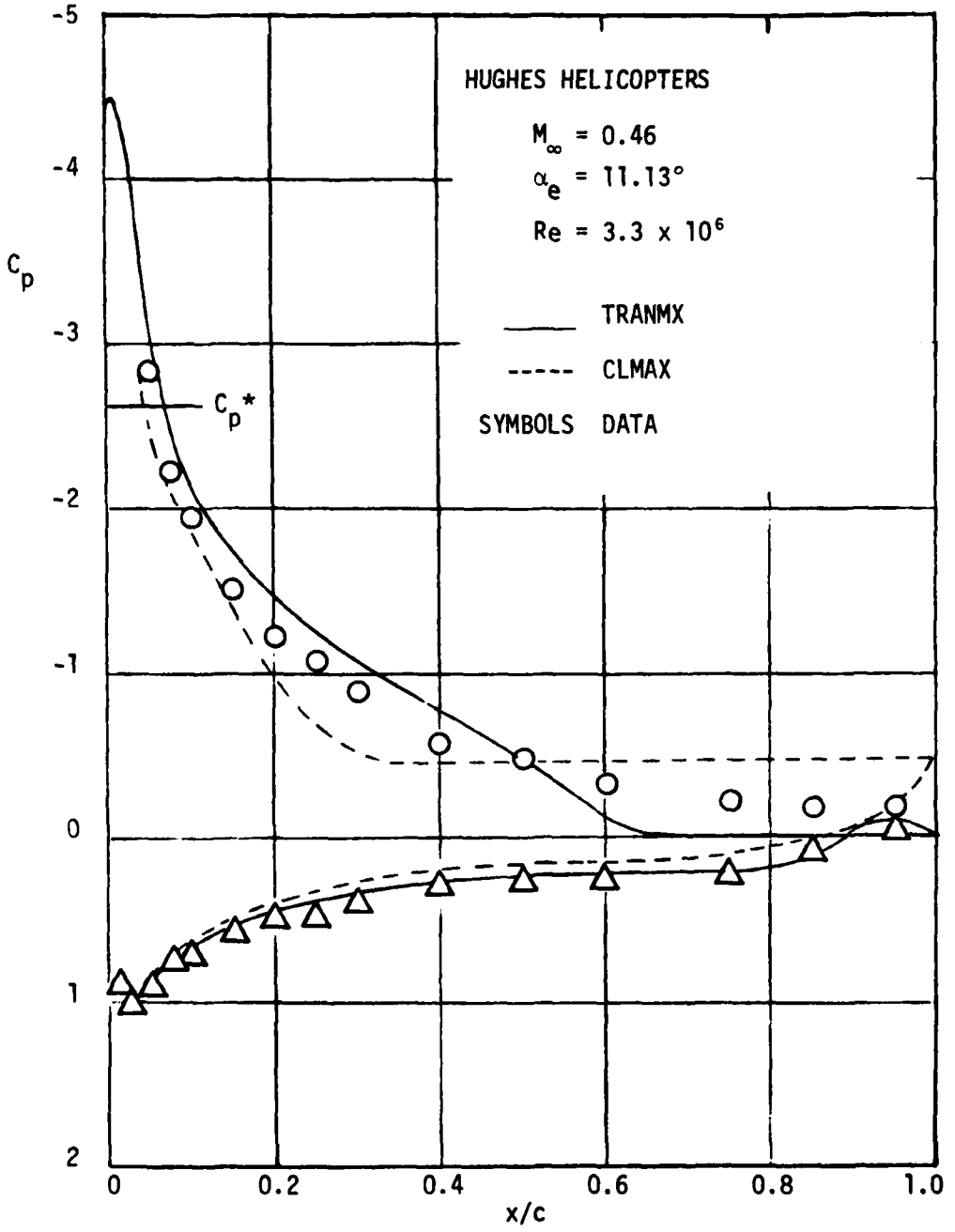

(c)

Figure 10. Concluded.

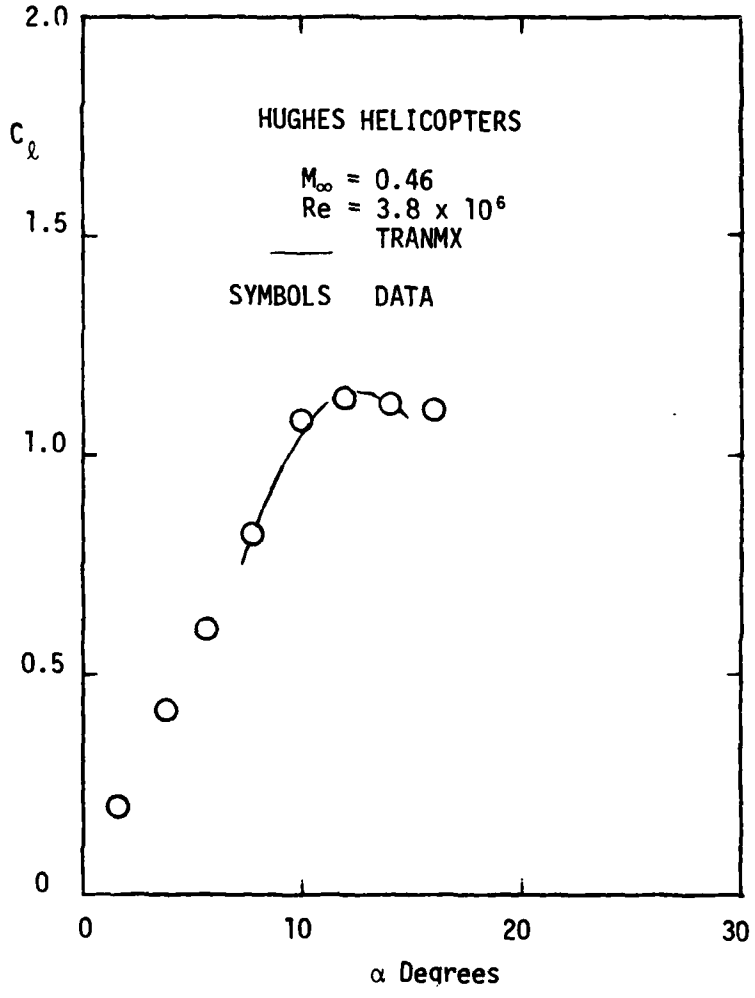

Figure 11. C_ℓ - α Curve for a Hughes Helicopters Company Airfoil.

Another helicopter section, the A1 airfoil, results are compar' in Figures 12, 13 and 14. The data was collected by Hicks and McCroskey (Ref. 11) in the Ames 2' x 2' Transonic Wind Tunnel with the model airfoil chord of 0.5 feet. Among a wide range of test conditions, only the Mach numbers of 0.5 and 0.6 are chosen owing to the present interest. The C_ℓ - α curve shown in Figure 12 can be divided into three regions. The flow in the first region, $\alpha < 8°$, can be characterized by the trailing-edge separation. The lift, C_ℓ, varies nearly linearly with respect to α in this region. The next region represents the flow for angles of attack from 8° to α_{CLMAX}. The boundary layer in this region separates at the foot of the shock and thus blunts the shock front. In this region a combination of shock separation and trailing-edge separation are present. C_ℓ varies gradually in this region until the catastrophic leading-edge separation brings the lift down sharply in the third region.

The results are in good agreement with experiment in region I. The calculated C_ℓ is much higher than the experimental data in the region II, although the general trend of C_ℓ - α curve is in close agreement with the experiment. The lower experimental C_ℓ is due to the shock boundary layer separation which the present method currently cannot predict. The pressure distributions shown in Figures 13 and 14 correlate very well with the experimental data. It is interesting to note, in Figure 14, the unsteady behavior of the pressure in the leading-edge region. This unsteadiness may indicate the temporary presence of shock boundary layer separation bubble which was mentioned earlier.

As we have seen so far in this section, the new calculation method performs very well for all the cases tested. The minor discrepancies which exist in some of the comparisons are attributed to the calculation method's own limitations rather than inconsistent performance. Misleading high lift, which is likely to happen when the method does not detect the shock boundary layer separation, can be easily noted by a careful analysis of the result. One obvious clue may be the unrealistically high local speed, say, $M > 1.4$, since the boundary layer through this shock is not likely to remain attached.

The main difficulty in verifying the calculation method has been the lack of quality transonic flow data. Most of the available data are limited to the case of no or small separated flow regions. In some cases, e.g., the A1 airfoil, the angle-of-attack correction due to tunnel blockage effect is so large (for $M_\infty = 0.6$, $\Delta\alpha \approx \alpha$) that the credibility of the data is in serious doubt. More reliable high Mach number flow data with a substantial region of reversed flow are desired for the future improvement of the calculation method.

---

(11) Hicks, R.M. and McCroskey, W.J., "An Experimental Evaluation of a Helicopter Rotor Section Designed by Numerical Optimization", NASA TM-78622, March 1980.

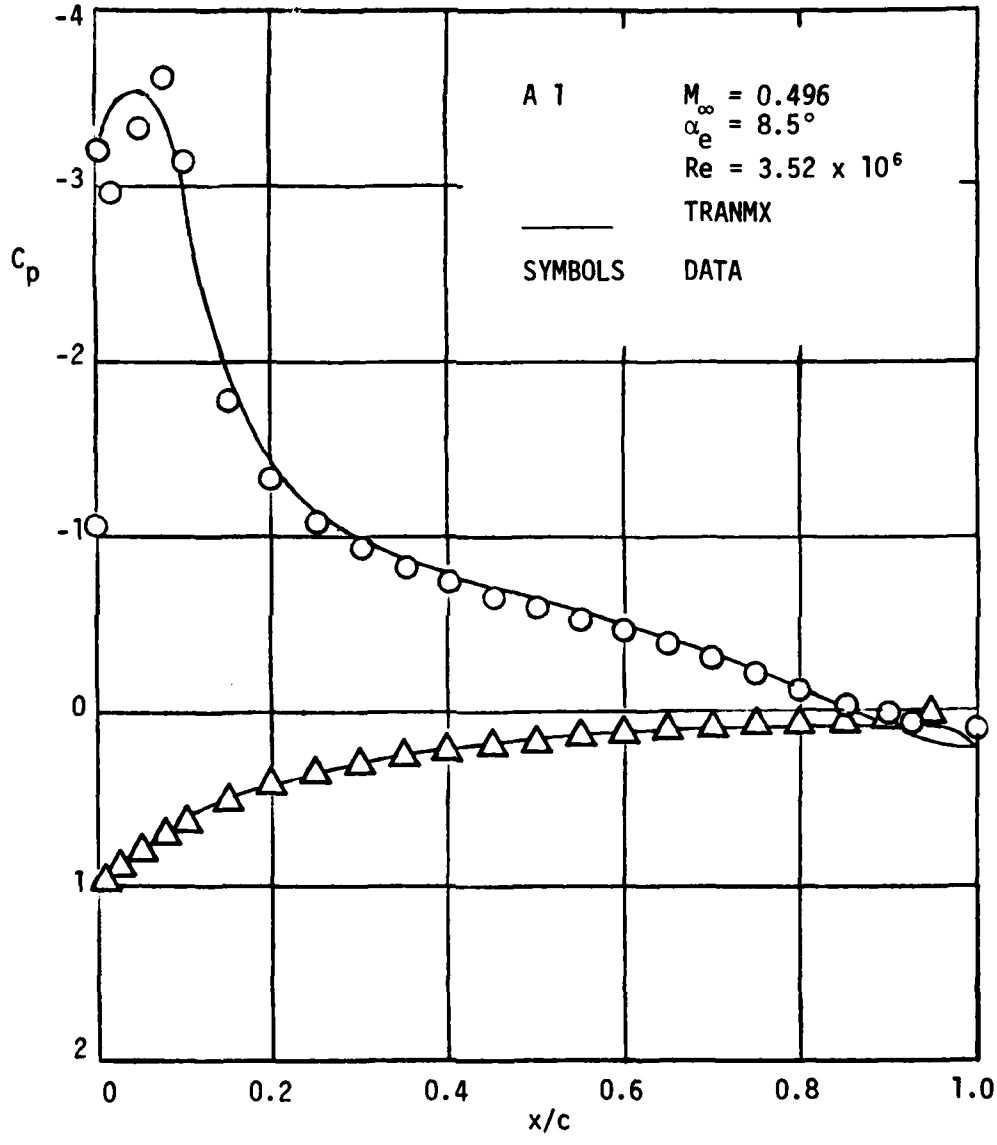

Figure 12. Pressure Distribution along an A1 Airfoil for M_∞ = 0.496; α = 8.5°.

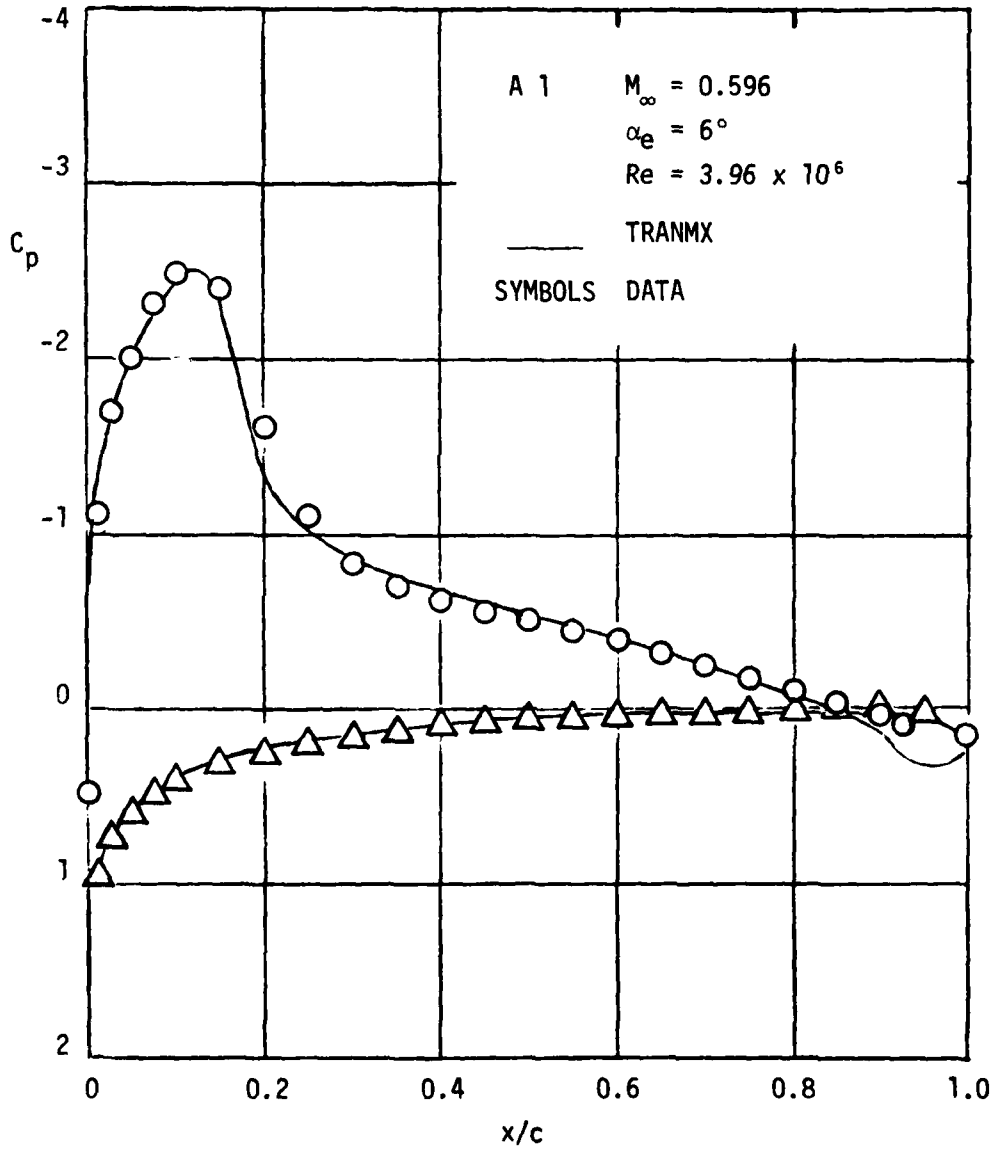

Figure 13. Pressure Distribution along an A1 Airfoil for M_∞ = 0.596; α = 6°.

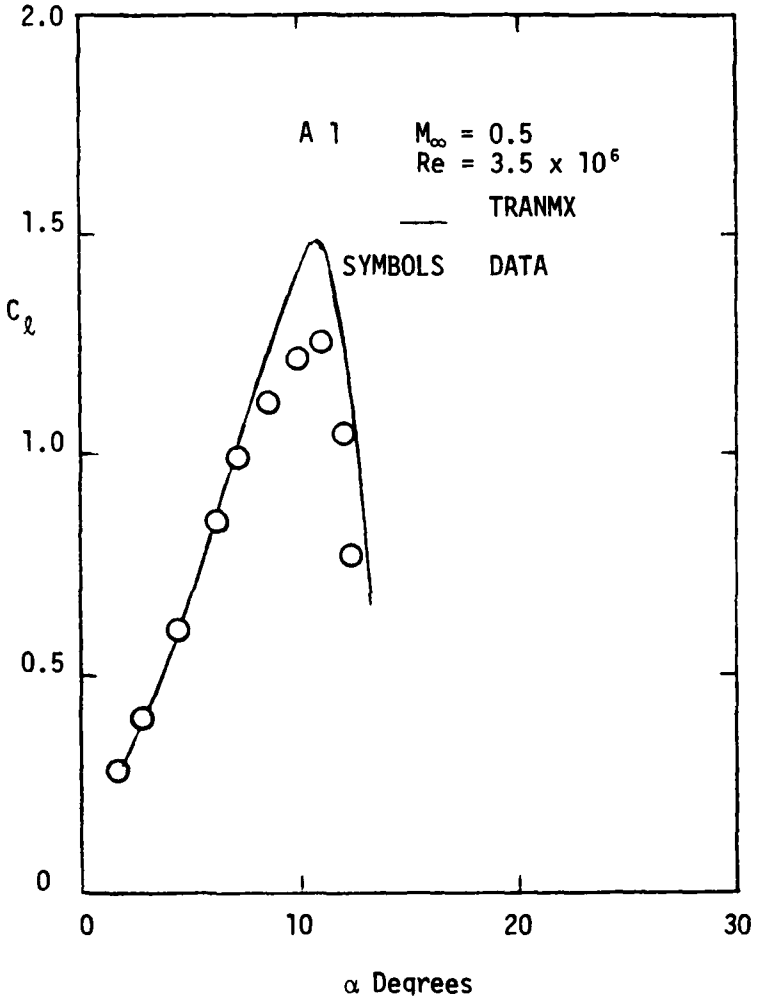

Figure 14. C_ℓ - α Curve for A1 Airfoil.

4.0 CONCLUSIONS

An analysis method for transonic trailing-edge type separated flow has been successfully demonstrated in comparison with experimental data. Predicted C_ℓ - α behavior is in good agreement with experiment for several different airfoil types at Mach numbers approaching 0.6. At higher Mach numbers inspection of the local Mach number distribution usually suggests separation as a result of strong shocks. While the program is not currently capable of modelling this phenomenon, it can be used as a predictive tool to indicate when shock/boundary layer separation can be expected.

The main advantage of this method over other existing methods is that the present scheme with its simple wake model allows computations for massive separation. It also can be extended to the three-dimensional case where, as previously cited, alternate methods are limited to two-dimensional flow.

5.0 REFERENCES

1. Hicks, R., Private Communication, 1977.

2. Diewert, G.S., "Computation of Separated Transonic Turbulent Flows", AIAA Paper No. 75-829, June 1975.

3. Barnwell, R.W., "A Potential Flow/Boundary Layer Method for Calculating Subsonic and Transonic Airfoil Flow with Trailing-Edge Separation", NASA TM-81850, June 1981.

4. Cousteix, J., AFOSR-HTTM-Stanford Conference on: Complex Turbulent Flows, Comparison of Computation and Experiment - Volume I, Stanford University, September 1981.

5. Dvorak, F.A., Maskew, B. and Rao, B.M., "An Investigation of Separation Models for the Prediction of $C_{\ell_{max}}$", Final Technical Report, Contract DAAG29-76-C-0019, Prepared for the U.S. Army Research Office, Research Triangle Park, N.C., April 1979.

6. Jameson, A., "Numerical Computation of Transonic Flows with Shock Waves", International Union of Theoretical and Applied Mechanics, Springer Verlag New York, Inc., September 1975, pp. 384-414.

7. Burne, G.W. and Manke, J.W., "An Improved Version of the NASA Lockheed Multielement Airfoil Analysis Computer Program", NASA CR-15323, March 1978, pp. 69-87.

8. Green, J.E., Weeks, D.J. and Brooman, J.W.F., "Prediction of Turbulent Boundary Lyaers and Wakes in Compressible Flow by a Lag-Entrainment Method", Royal Aircraft Establishment TR-72231, December 1972.

9. Rogers, E.O., "Numerical Solution of Subcritical Flow Past Airfoils", NSRDC Report 4112, May 1973.

10. Dvorak, F.A. and Woodward, F.A., "A Viscous/Potential Flow Interaction Analysis Method for Multi-Element Infinite Swept Wings; Volume I", NASA CR-2476, November 1974.

11. Hicks, R.M. and McCroskey, W.J., "An Experimental Evaluation of a Helicopter Rotor Section Designed by Numerical Optimization", NASA TM-78622, March 1980.